Supporting Information (SI)

An new metal-organic framework based on rare $[Zn_4F_4]$ cores for efficient separation of C_2H_2

Wen-Juan Shi,[a] Yong-Zhi Li,*[a, b] Jing Chen,[c] Run-Han Su,[a] Lei Hou,*[a] Yao-Yu Wang[a] and Zhonghua Zhu[d]

[a]Key Laboratory of Synthetic and Natural Functional Molecule of the Ministry of Education, Shaanxi Key Laboratory of Physico-Inorganic Chemistry, College of Chemistry & Materials Science, Northwest University, Xi'an *710069*, P. R. China.

[b]School of Materials and Physics, China University of Mining & Technology, Xuzhou 221116, PR China

[c]Shaanxi Yanchang Petroleum (Group) Co., Ltd., Xi'an 710069, P. R. China.

[d]School of Chemical Engineering, The University of Queensland, Brisbane, 4072, Australia.

*To whom correspondence should be addressed. E-mail: yzli1120@foxmail.com (Yong-Zhi Li), lhou2009@nwu.edu.cn (Lei Hou).

Materials and general methods.

All solvents and organic ligand 1, 4-benzenedicarboxylate (H_2BDC) for synthesis were purchased commercially. Elemental analyses of C, H, and N were determined with a Perkin-Elmer 2400C elemental analyzer. Powder X-ray diffraction (PXRD) data were recorded on a Bruker D8 ADVANCE X-ray powder diffractometer (Cu Kα, λ = 1.5418 Å). Thermalgravimetric analyses (TGA) were carried out in a nitrogen stream using a Netzsch TG209F3 equipment at a heating rate of 10 °C min^{-1}. XPS (X-ray photoelectron spectroscopy) spectra were tested on a ULVAC PHI5000 Versa ProbeIII equipment. Adsorption measurements were performed with an automatic volumetric sorption apparatus (Micrometrics ASAP 2020M). Breakthrough experiments were performed on a Quantachrome dynaSorb BT equipment.

Synthesis of $[(CH_3)_2NH_2]_2\cdot[Zn_4(\mu_3\text{-}F)_4(\mu_2\text{-}F)_2(BDC)_2]\cdot 4(DMF)\cdot 4(H_2O)$ (1).

The mixture containing 0.029 g $ZnSO_4\cdot 7H_2O$ (0.1 mmol), 0.017 g H_2BDC (0.1 mmol), 3 mL CH_3OH, 7 mL DMF and one drop of HF was sealed in a vessel (25 mL). The vessel was heated to 120 °C at a heating rate of 4 °C h^{-1} for 72 h, and then cooled to RT within 8 h to give colorless massive crystals (yield: 72%, based on $ZnSO_4$). Anal. Calcd for $C_{32}H_{63}F_6N_6O_{16}Zn_4$: C, 33.03; H, 5.46; N, 7.22%. Found: C, 32.82; H, 5.69; N, 3.45%.

X-ray crystallography.

A Bruker Smart Apex II CCD detector was used to collect the single crystal data at 150(2) K using Mo Kα radiation (λ = 0.71073 Å). The structure was solved by direct methods and refined by full-matrix least-squares refinement based on F^2 with the SHELXTL program.The non-hydrogen atoms were refined anisotropically with the hydrogen atoms added at their geometrically ideal positions and refined isotropically. As the disordered solvent DMF molecules in the structure cannot be located, the SQUEEZE routine of Platon program was applied in refining. The formula of complex was got by the single crystal analysis together with elemental microanalyses and TGA data. Relevant crystallographic results are listed in Table S1. Selected bond lengths and angles are provided in Table S2.

Breakthrough measurements.

The gas breakthrough separation experiment was carried out at 273 K and 298 K in a Quantachrome dynaSorb BT equipments fixed-bed reactor. In a typical breakthrough experiment using the mixture of C_2H_2-CH_4-Ar (5%-5%-90%) and C_2H_2-CO_2-Ar (5%-5%-90%), **1a** powder (1.0g) was packed into a packed column (about 4.2 × 80 mm^2). The adsorbent was activated at 423 K for 12 hours, and argon flow (7 mL min^{-1}) was introduced after the activation process to purge the adsorbent. The gas mixture of C_2H_2-CH_4-Ar (5%-5%-90%) then flows into the column at 7 mL min^{-1}. Gas chromatograph is used to monitor the outlet gas of the breakthrough column. After the breakthrough experiment, the sample was regenerated with argon flow (7 mL min^{-1}) at 353 K for 0.5 hours. The complete breakthrough of C_2H_2 and CH_4 was indicated by the downstream gas composition reaching that of the feed gas.

On the basis of the mass balance, the gas adsorption capacities can be determined as follows:

$$q_i = \frac{C_i V}{22.4 \times m} \times \int_0^t (1 - \frac{F}{F_0}) dt$$

Where q_i is the equilibrium adsorption capacity of gas i (mmol g^{-1}), C_i is the feed gas concentration, V is the volumetric feed flow rate (cm^3 min^{-1}), t is the adsorption time (min), F_0 and F are the inlet and outlet gas molar flow rates, respectively, and m is the mass of the adsorbent (g).

The separation factor (α) of the breakthrough experiment is determined as:

$$\alpha = \frac{q_A y_B}{q_B y_A}$$

in which y_i is the molar fraction of gas i (i = A, B) in the gas mixture.

GCMC simulation.

Grand canonical Monte Carlo (GCMC) simulations were performed for the gas adsorption in the framework by the Sorption module of Material Studio (Accelrys. Materials Studio Getting Started, release 5.0). The framework was considered to be rigid, and the optimized gas molecules were used. The partial charges for atoms of the framework were derived from

QEq method and QEq neutral 1.0 parameter. One unit cell was used during the simulations. The interaction energies between the gas molecules and framework were computed through the Coulomb and Lennard-Jones 6-12 (LJ) potentials. All parameters for the atoms were modeled with the universal force field (UFF) embedded in the MS modeling package. A cutoff distance of 12.5 Å was used for LJ interactions, and the Coulombic interactions were calculated by using Ewald summation. For each run, the 3×10^6 maximum loading steps, 3×10^6 production steps were employed.

Fitting adsorption heat of pure component isotherms.

$$\ln P = \ln N + 1/T \sum_{i=0}^{m} a_i N^i + \sum_{i=0}^{n} b_i N^i \qquad Q_{st} = -R \sum_{i=0}^{m} a_i N^i$$

The virial expression was used to fit the combined isotherm data for **1a** at 273.15 and 298 K, where P is the pressure, N is the adsorbed amount, T is the temperature, ai and bi are virial coefficients, and m and N are the number of coefficients used to describe the isotherms. Q_{st} is the coverage-dependent enthalpy of adsorption and R is the universal gas constant.

Gas selectivity prediction via IAST.

The experimental isotherm data for pure gas were fitted using a dual Langmuir-Freundlich (L-F) model:

$$q = \frac{a_1 * b_1 * P^{c1}}{1 + b_1 * P^{c1}} + \frac{a_2 * b_2 * P^{c2}}{1 + b_2 * P^{c2}}$$

Where q and p are adsorbed amounts and the pressure of component i, respectively.

The adsorption selectivities for binary mixtures of C_2/CH_4, defined by

$$S_{i/j} = \frac{x_i * y_j}{x_j * y_i}$$

were respectively calculated using the Ideal Adsorption Solution Theory (IAST). Where x_i is the mole fraction of component *i* in the adsorbed phase and y_i is the mole fraction of component i in the bulk.

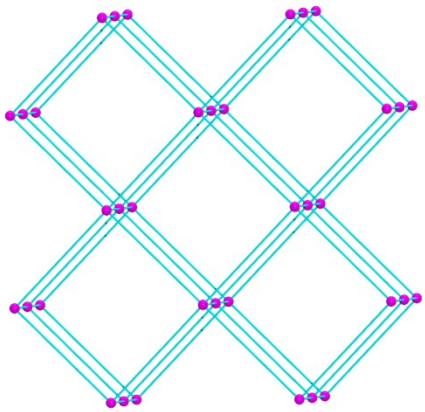

Fig. S1 Topological net of complex **1**.

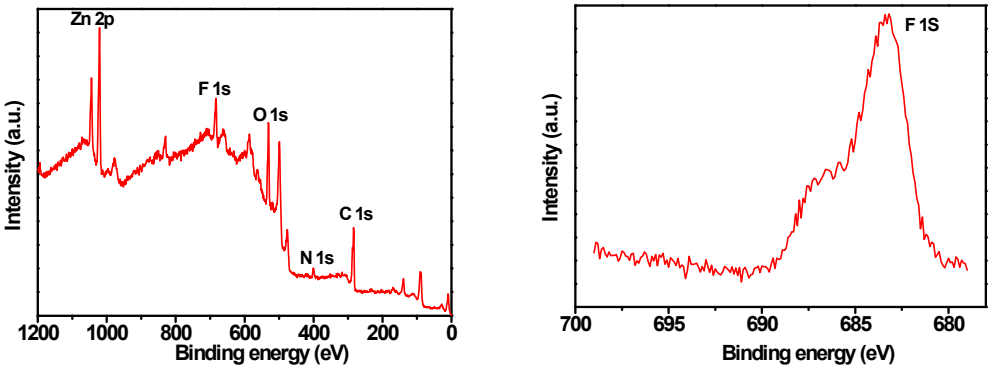

Fig. S2 XPS patterns of complex **1**: survey and F 1s.

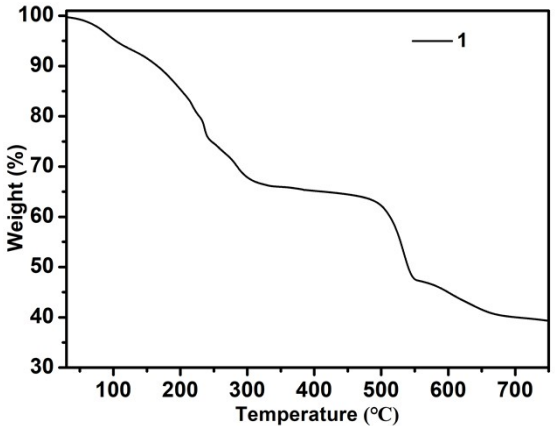

Fig. S3 TGA curve of complex **1**.

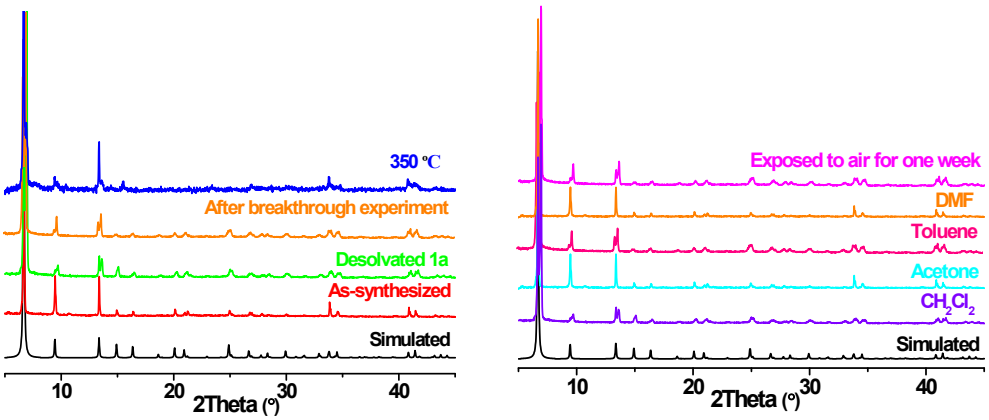

Fig. S4 PXRD patterns of complex **1** after treatment with different conditions.

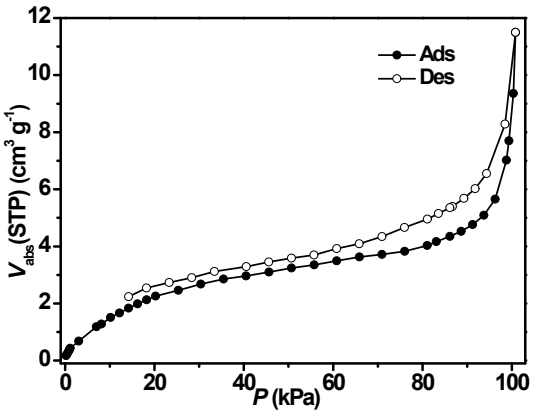

Fig. S5 Adsorption isotherm of complex **1** for N_2 at 77 K.

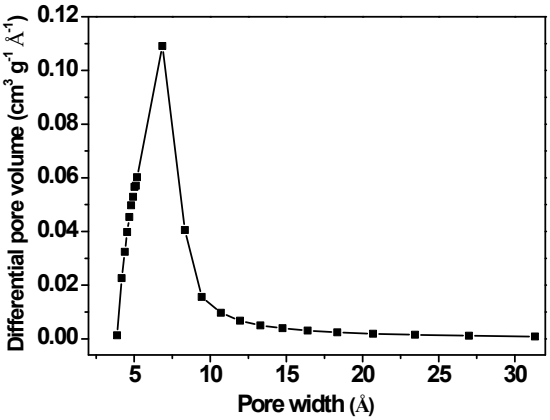

Fig. S6 Differential pore volume as a function of pore width calculated from the CO_2 adsorption isotherm at 195 K for **1a** using the Horvath-Kawazoe model.

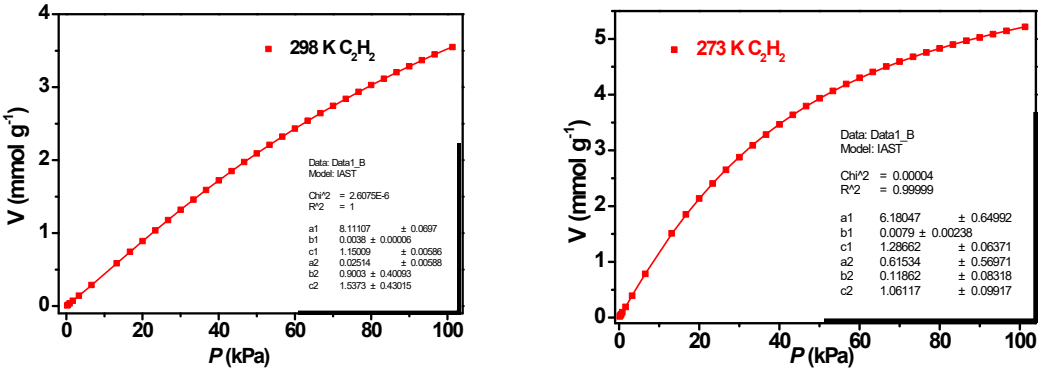

Fig. S7 C_2H_2 adsorption isotherms of **1a** fitted by dual L-F model.

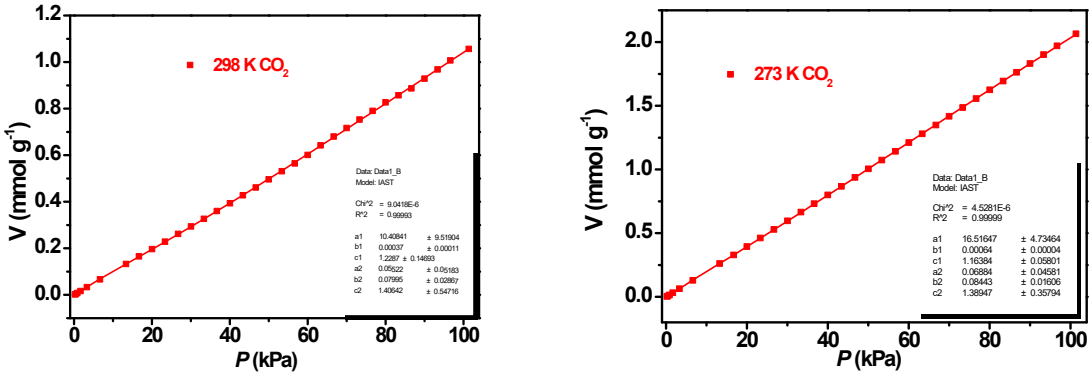

Fig. S8 CO_2 adsorption isotherms of **1a** fitted by dual L-F model.

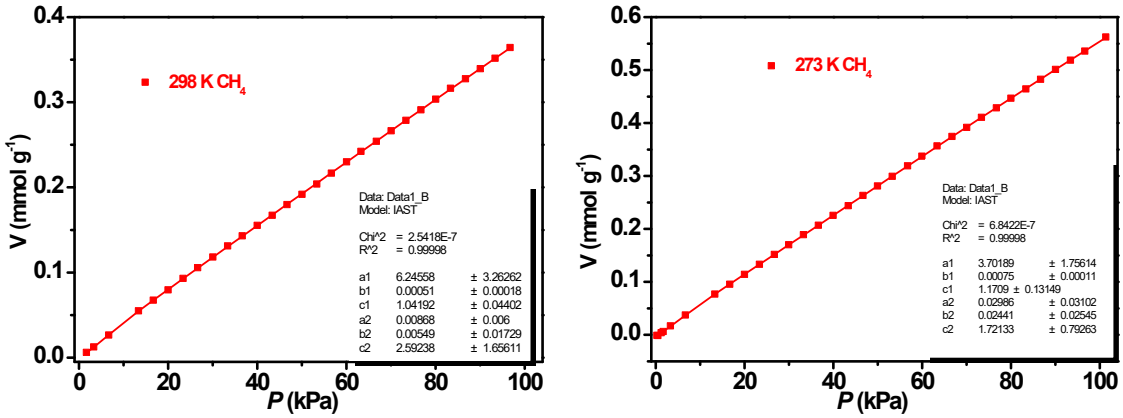

Fig. S9 CH_4 adsorption isotherms of **1a** fitted by dual L-F model.

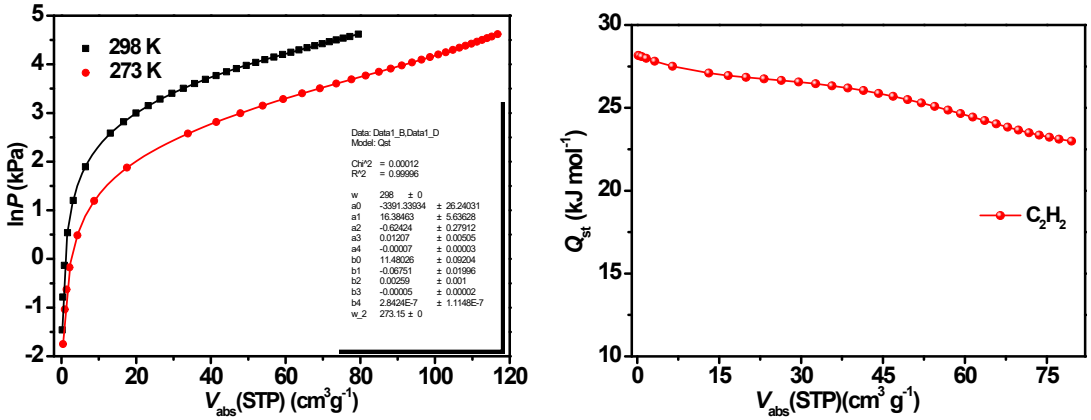

Fig. S10 Fitted C_2H_2 isotherms of **1a**, and the heat of adsorption (Q_{st}).

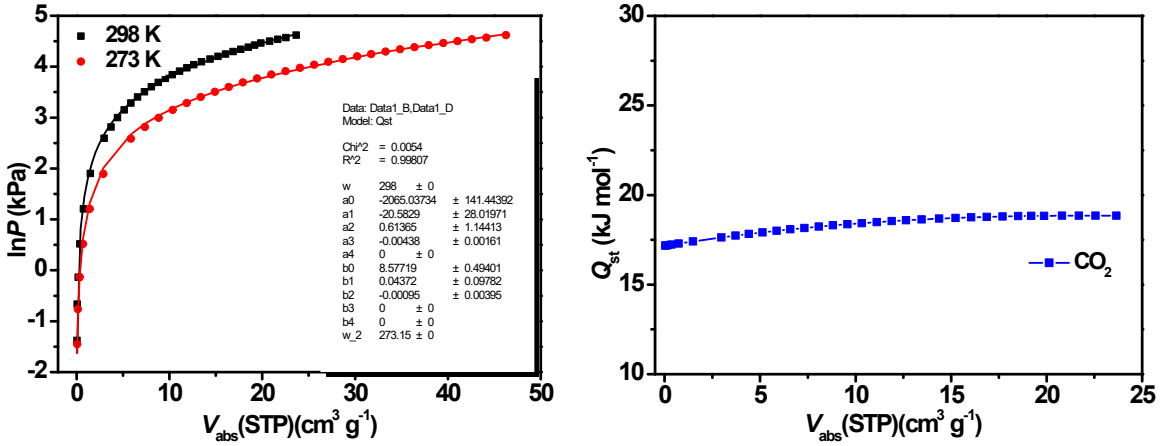

Fig. S11 Fitted CO_2 isotherms of **1a**, and the heat of adsorption (Q_{st}).

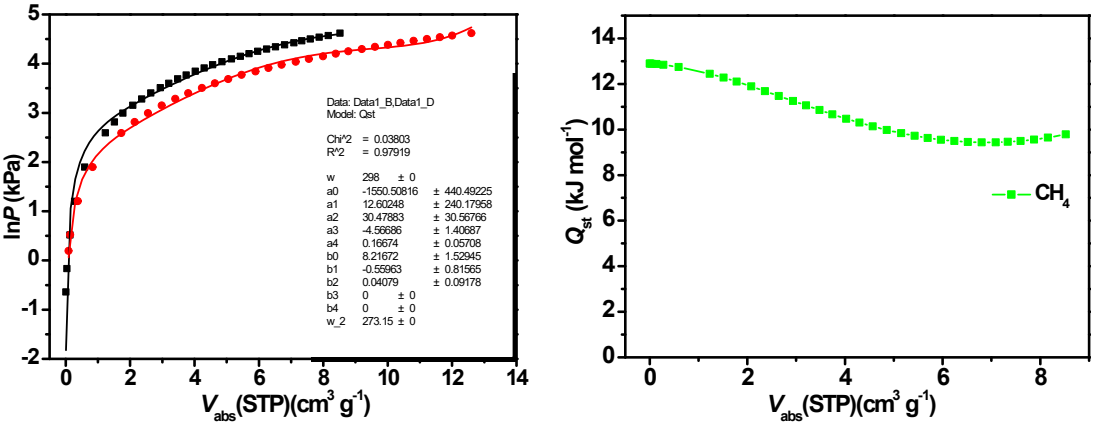

Fig. S12 Fitted CH_4 isotherms of **1a**, and the heat of adsorption (Q_{st}).

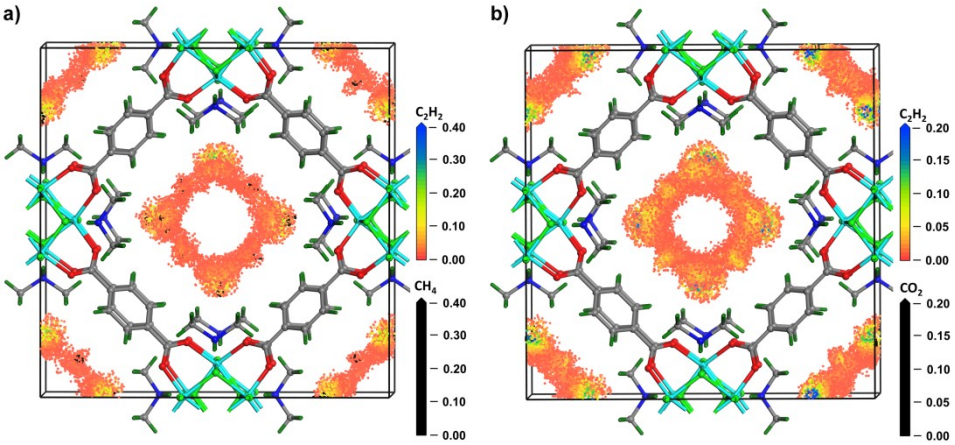

Fig. S13 Density contours in **1a**: a) C_2H_2 and CH_4; b) C_2H_2 and CO_2.

Table S1. Crystal Data and Structure Refinements for complex **1**.

Chemical formula	$C_{20}H_{24}F_6N_2O_8Zn_4$
Formula weight	795.89
T (K)	296(2) K
Crystal system	Tetragonal
Space group	*I4/mmm*
a/b (Å)	18.7279(4)/18.7279 (14)
c (Å)	11.8716 (6)
$\alpha/\beta/\gamma$ (°)	90/90/90
V (Å^3)	4163.8 (3)
Z	4
$D_{calcd.}$[g·cm^{-3}]	1.270
μ (mm^{-1})	2.334
Reflns collected/unique/R_{int}	34450/1131/0.0398
Goof	1.106
R_1[a], wR_2[b] [I > 2σ]	R_1 = 0.0161, wR_2 = 0.0407
R_1[a], wR_2[b] (all data)	R_1 = 0.0177, wR_2 = 0.0416

[a]$R_1 = \Sigma(|F_o|-|F_c|)/\Sigma|F_o|$. [b]$R_2 = [\Sigma w(F_o^2 - F_c^2)^2/\Sigma w(F_o^2)^2]^{1/2}$.

Table S2. Selected bond lengths [Å] and angles [°] for complex **1**.

Zn(1)-F(2)	1.9262(3)	F(2)-Zn(1)-F(1)#2	94.68(5)
Zn(1)-O(1)	2.0194(10)	O(1)-Zn(1)-F(1)#2	160.25(4)
Zn(1)-O(1)#1	2.0195(10)	O(1)#1-Zn(1)-F(1)#2	88.94(4)
Zn(1)-F(1)#2	2.1148(7)	F(2)-Zn(1)-F(1)#3	94.68(5)

Zn(1)-F(1)#3	2.1148(7)	O(1)-Zn(1)-F(1)#3	88.95(4)
Zn(1)-F(1)	2.1191(11)	O(1)#1-Zn(1)-F(1)#3	160.25(4)
F(1)-Zn(1)#2	2.1148(7)	F(1)#2-Zn(1)-F(1)#3	74.22(5)
F(1)-Zn(1)#3	2.1148(7)	F(2)-Zn(1)-F(1)	174.02(6)
F(2)-Zn(1)#6	1.9262(3)	O(1)-Zn(1)-F(1)	86.65(3)
F(2)-Zn(1)-O(1)	96.95(4)	O(1)#1-Zn(1)-F(1)	86.65(3)
F(2)-Zn(1)-O(1)#1	96.95(4)	F(1)#2-Zn(1)-F(1)	80.57(4)
O(1)-Zn(1)-O(1)#1	105.36(6)	F(1)#3-Zn(1)-F(1)	80.57(4)

Symmetry codes: #1 -x, y, z; #2 -y+1/2, x+1/2, -z+3/2; #3 y-1/2, -x+1/2, -z+3/2; #4 y-1/2, x+1/2, -z+3/2; #5 -y+1, -x+1, z; #6 x, y, -z+2.

Table S3. Summary of $[M_4(\mu_3\text{-}F)_4]$ cubane complexes.

	M	Formula	Ref.
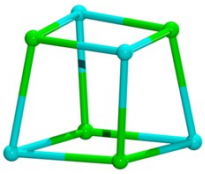 $[M_4(\mu_3\text{-}F)_4]$ cubanes	Co^{2+}	$[Co_4F_4(L)_{12}.](BF_4)_4$, L = N-ethylimidazole or N-propylimidazole.	S1
	Ca^{2+}	$[(15\text{-crown-}5)_3(Ca_4F_4)(PF_6)CH_3CN](PF_6)_3$	S2
	Ni^{2+}	$[Ni_4F_4\{S(pz)_2\}_4(\mu\text{-}FAsF_4F)_2](AsF_6)_2{\cdot}4SO_2$	S3
	Re^{+}	$[Re(CO)_3F]_4{\cdot}4H_2O$	S4
	Rh^{+}	$[FRh(C_2H_4)(C_2F_4)]_4$	S5
	Pt^{4+}	$[(CH_3)_3PtF]_4$	S6

Table S4. Comparison of the Q_{st}, adsorption capacity and C_2H_2/CO_2 uptake ratios of **1a** with other MOF materials at 298 K.

MOF	C_2H_2 uptake ($cm^3\ g^{-1}$)	CO_2 uptake ($cm^3\ g^{-1}$)	C_2H_2/CO_2 uptake ratios	Q_{st} (KJ mol^{-1})	Ref
1a	79.5	23.6	3.37	28.2	
JXNU-5a	55.9	34.8	1.61	32.9	S7
Zn-MOF-74	123.8	121.4	1.02	24.0	S8
FJU-22a	114.8	111.3	1.03	/	S9
NKMOF-1-Ni	61.0	51.1	1.19	60.3	S10
UTSA-74a	107.4	70.9	1.51	31	S11
Cd(dtztp)	80.1	64.3	1.25	25	S12
UTSA-300a	68.9	3.25	21	57.6	S13
TIFSIX-2-Ni-i	94.3	101.7	0.93	40	S14
ATC-Cu	112.2	80.8	1.39	79.1	S15
ZrT-1-tetrazol	57.7	35.1	1.64	33.3	S16

$[Ni_3(HCOO)_6]$	53.4	34	1.57	40.9	S17
IPM-101	57.1	68.1	0.84	43.7	S18
TCuCl	67.2	44.8	1.5	41	S19
SNNU-16	46	37.2	1.24	52.6	S20
FJU-89a	101.4	61.1	1.66	31.0	S21
$Ni_2(BTEC)(bipy)_3$	76.8	13.0	5.9	19.8	S22

Table S5. Comparison of the Q_{st} and C_2H_2/CO_2 Selectivity of **1a** with other MOFs at 298 K.

MOF	C_2H_2 Q_{st} (KJ mol^{-1})	C_2H_2/CO_2 Selectivity	Ref.
1a	28.1	4.12	This work
UTSA-300a	57.6	21	S13
SNNU-16	52.6	2	S20
[Ni(dpip)]	41.7	2	S23
TIFSIX-2-Ni-i	40	6.1	S14
ZrT-1-tetrazol	33.3	2.83	S16
FJU-36a	32.9	2.8	S24
JXNU-5a	32.9	5	S7
FJU-6-TATB	29	3.1	S25
FJU-99a	28	2.2	S26
Cd-dtztp	25	2	S27
SNNU-27-Fe	24.1	2	S28
PCM-48	23.6	4.3	S29

References.

[S1] J. C. Jansen, H.van Koningsveld and J. Reedijk, *Nature*, 1977, **269**, 318-319.

[S2] E. N. Keyzer, P. D. Matthews, Z. Liu, A. D. Bond, C. P. Grey and D. S. Wright, *Chem. Commun*., 2017, **53**, 4573-4576.

[S3] M. Schröter, E. Lork and R. Mews, *Z. Anorg. Allg. Chem*. 2005, **631**, 1609-1614.

[S4] E. Horn and M. R. Snow, *Aust. J. Chem*., 1981, **34**, 737-473.

[S5] R. R. Burch, R. L. Harlow and S. D. Ittel, *Organometallics*, 1987, **6**, 982-987.

[S6] H. Donath, E. V. Avtomonov, I. Sarraje, K.-H. von Dahlen, M. El-Essawi, J. Lorbeth, B.-S. Seo, *J. Organomet.Chem*., 1998, **559**, 191-196.

[S7] R. Liu, Q.-Y. Liu, R. Krishna, W. Wang, C.-T. He and Y.-L. Wang, *Inorg. Chem*., 2019, **58**, 5089-5095.

[S8] S. Xiang, W. Zhou, Z. Zhang, M. A. Green, Y. Liu and B. Chen, *Angew. Chem., Int. Ed*.,

2010, **49**, 4615-4618.

[S9] Z. Yao, Z. Zhang, L. Liu, Z. Li, W. Zhou, Y. Zhao, Y. Han, B. Chen, R. Krishna and S. Xiang, *Chem. - Eur. J.*, 2016, **22**, 5676-5683.

[S10] Y.-L. Peng, T. Pham, P. Li, T. Wang, Y. Chen, K.-J. Chen, K. A. Forrest, B. Space, P. Cheng, M. J. Zaworotko and Z. Zhang, *Angew. Chem., Int. Ed*., 2018, **57**, 10971-10975.

[S11] F. Luo, C. Yan, L. Dang, R. Krishna, W. Zhou, H.Wu, X. Dong, Y. Han, T.-L. Hu, M. O'Keeffe, L. Wang, M. Luo, R.-B. Lin and B. Chen, *J. Am. Chem. Soc.*, 2016, **138**, 5678-5684.

[S12] G.-D. Wang, Y.-Z. Li, W.-J. Shi, L. Hou, Z. Zhu and Y.-Y. Wang, *Inorg. Chem. Front.*, 2020, **7**, 1957-1964.

[S13] R.-B. Lin, L. Li, H. Wu, H. Arman, B. Li, R.-G. Lin, W. Zhou and B. Chen, *J. Am. Chem. Soc*., 2017, **139**, 8022-8028.

[S14] M. Jiang, X. Cui, L. Yang, Q. Yang, Z. Zhang, Y. Yang and H. Xing, *Chem. Eng. J.*, 2018, **352**, 803-810.

[S15] Z. Niu, X. Cui, T. Pham, G. Verma, P. C. Lan, C. Shan, H. Xing, K. A. Forrest, S. Suepaul, B. Space, A. Nafady, A. M. Al-Enizi and S. Ma, *Angew. Chem. Int. Ed*. 2021, **60**, 5283-5288.

[S16] W. Fan, S. B. Peh, Z. Zhang, H. Yuan, Z. Yang, Y. Wang, K. Chai, D. Sun and D. Zhao, *Angew. Chem. Int. Ed*., 2021, **60**, 17338-17343.

[S17] L. Zhang, K. Jiang, J. Zhang, J. Pei, K. Shao, Y. Cui, Y. Yang, B. Li, B. Chen and G. Qian, *ACS Sustainable Chem. Eng*., 2019, **7**, 1667-1672.

[S18] S. Sharma,S. Mukherjee, A. V. Desai, M. Vandichel, G. K. Dam, A. Jadhav, G. Kociok-Köhn, M. J. Zaworotko and S. K. Ghosh, *Chem. Mater*., 2021, **33**, 5800-5808.

[S19] S. Mukherjee, Y. He, D. Franz, S.-Q. Wang, W.-R. Xian, A. A. Bezrukov, B. Space, Z. Xu, J. He and M. J. Zaworotko, *Chem. Eur. J.*, 2020, **26**,4923-4929.

[S20] H.-P. Li, Z.-D. Dou, Y. Wang, Y. Y. Xue, Y. P. Li, M.-C. Hu, S.-N. Li, Y.-C. Jiang and Q.-G. Zhai, *Inorg. Chem*., 2020, **59**, 16725-16736

[S21] Y. Ye, S. Chen, L. Chen, J. Huang, Z. Ma, Z. Li, Z. Yao, J. Zhang, Z. Zhang and S. Xiang, *ACS Appl. Mater. Interfaces*, 2018, **10**, 30912-30918.

[S22] Y. Du, Y. Chen, Y. Wang, C. He, J. Yang, L. Li and J. Li, *Separ. and Purif. Techno.*,

2021, **256**, 117749.

[S23] Y.-Z. Li, G.-D. Wang, L.-N. Ma, L. Hou, Y.-Y. Wang and Z. Zhu, *ACS Appl. Mater. Interfaces*, 2021, **13**, 4102-4109.

[S24] L. Liu, Z. Yao, Y. Ye, L. Chen, Q. Lin, Y. Yang, Z. Zhang and S. Xiang, *Inorg. Chem*., 2018, **57**, 12961-12968.

[S25] L. Liu, Z. Yao, Y. Ye, Y. Yang, Q. Lin, Z. Zhang, M. O'Keeffe and S. Xiang, J. Am. Chem. Soc., 2020, **142**, 9258-9266.

[S26] T. Chen, Y. Ye, M. Yin, L. Chen, Z. Ke, J. Guo, M. Zhang, Z. Yao, Z. Zhang and S. Xiang, *Cryst. Growth Des*., 2020, **20**, 2099-2105.

[S27] G.-D. Wang, Y.-Z. Li, W.-J. Shi, L. Hou, Z. Zhu and Y.-Y. Wang, *Inorg. Chem. Front*., 2020, **7**, 1957-1964.

[S28] Y.-Y. Xue, X.-Y. Bai, J. Zhang, Y. Wang, S.-N. Li, Y.-C. Jiang, M.-C. Hu and Q.-G. Zhai, *Angew. Chem. Int. Ed*., 2021, **60**, 10122-10128.

[S29] J. E. Reynolds, K. M. Walsh, B. Li, P. Kunal, B. Chen and S. M. Humphrey, *Chem. Commun*., 2018, **54**, 9937-9940.